Preprints, 10th IFAC International Symposium on
Advances in Automotive Control
Columbus, Ohio, USA, August 28-30, 2022

Observer-based Purge Estimation for Robust Air Fuel Ratio Control of Internal Combustion Engines

Yongsoon Yoon

Department of Mechanical Engineering
Oakland University
Rochester, MI 48309 USA

Abstract: This paper presents a purge estimation method for a robust air fuel ratio control of internal combustion engines. The air fuel ratio control is a primary emission control mechanism of gasoline engines, and purge is one of the most critical disturbances that can lead to significant air fuel ratio excursions. In this work, Luenberger-like unknown input observers are proposed to estimate purge flow rate and purge fuel fraction using existing sensors available in production engine management systems. The convergence properties of the proposed observers are investigated analytically and numerically. The estimation method allows to improve accuracy of the air fuel ratio control by compensating for the purged fuel, thereby it allows aggressive purge in a wide range of operational conditions to meet stringent evaporative emission standards.

Keywords: Evaporative emission control systems, Luenberger observer, air-fuel ratio control, internal combustion engines.

1. INTRODUCTION

Since the inception of evaporative emission standards, an evaporative emission control system, shortly an EVAP system, has been a standard feature of gasoline-powered vehicles. The EVAP system (see Fig. 1) prevents fuel vapors in the fuel tank from escaping into the atmosphere, Goto et al. (1982). Because of its high volatility, gasoline fuel is easily vaporized in hot conditions. The charcoal canister absorbs and stores fuel vapor. However, because the load capacity of the charcoal canister is limited, it is purged to the intake manifold periodically. While the purge valve opens, a fresh air stream is drawn through the vent line, and it traps and delivers fuel vapor from the surface of the charcoal to the intake manifold. Due to more stringent regulations on evaporative emission and test procedures mandated by the regulatory body, more aggressive purge strategies, such as a high purge rate during idle, are required to deplete fuel vapors stored in the charcoal canister, Grieve and Himes (2000).

However, purge gas is one of the most detrimental disturbance factors to an air fuel ratio (AFR) control which is a primary emission control mechanism of gasoline engines. In order to maintain high conversion efficiency of a three-way-catalyst (TWC), AFR is controlled in a narrow band near the stoichiometric value (i.e. 14.65 for pure gasoline) where all regulated emissions including hydrocarbon (HC), carbon monoxide (CO) and nitrogen oxides (NOx) are converted into non-toxic gases simultaneously with high conversion efficiency using an exhaust gas oxygen (EGO) sensor feedback, Heywood (1998).

Although purge valve opening strategies are available, purge brings significant uncertainties into the AFR control. First, the purge flow rate is uncertain due to complicated turbulence around the small purge valve. Second, purge gas is a mixture of air and fuel, and its composition is uncertain due to the large variability of gasoline vapor pressure and temperature conditions of the fuel tank. Unless these uncertainties are estimated accurately, and the fuel amount to be injected is compensated correctly, aggressive vapor purge may lead to significant AFR excursions due to low feedback control bandwidth, and ultimately significant increase in tailpipe emissions and degradation of driveability, Grieve and Himes (2000).

In literature, there has been much effort to estimate the purge flow rate and purge fuel fraction, and compensate for the fuel amount to be injected during purge events. Yoo et al. (1999) developed a physics-based carbon canister model and use the model for the AFR control in an open-loop manner. Grieve and Himes (2000) proposed a virtual hydrocarbon sensor based on an open-loop vapor purge model. Aswani et al. (2009) developed a dual-mode observer to estimate the vapor purge composition during closed-loop AFR control and open-loop AFR control separately. Recently, Corvino et al. (2014) proposed a high gain observer to estimate the AFR of purge gas, and Zamanian et al. (2014) proposed a steady-state fueling compensation method during purge events using an extra hydrocarbon sensor in the purge line.

In this work, Luenberger-like unknown input observers (UIOs) are proposed for purge estimation, which are feasible in production engine management systems (EMS) without any extra sensors. This work is motivated from unknown input observer-based engine charge flow estimation in Stotsky and Kolmanovsky (2002); Andersson and Eriksson (2005); Leroy et al. (2007); Hassani Monir et al. (2015); Wang et al. (2016). These works include a high gain observer, Luenberger-like observer, sliding mode observer, and extended Kalman filter, respectively, to estimate uncertain volumetric efficiency of internal combustion engines for an accurate feedforward AFR control. This paper is concerned with Luenberger-like UIOs to estimate the uncertain purge flow rate and purge fuel fraction to improve

⋆ Email address: yongsoonyoon@oakland.edu.

robustness of the AFR control, and their asymptotic convergence properties are investigated.

The remainder of this paper is outlined as follows: Sec. 2 presents mathematical models of intake manifold breathing dynamics and charge fuel fraction dynamics. Sec. 3 derives Luenberger-like observers for estimation of uncertain purge flow rate and unknown purge fuel fraction with the proofs of convergence. Then, Sec. 4 illustrates the effectiveness of the observers through numerical simulations. Lastly, Sec. 5 provides a brief summary and concluding remarks.

2. EVAP SYSTEM MODELING

A schematic of an internal combustion engine with an EVAP system is shown in Fig. 1. The symbols of p, T, W, F and u indicate pressure, temperature, flow rate, fuel fraction and valve input, respectively. The subscripts of a, th, m, p, egr, c, cyl and s indicate ambient, throttle valve, intake manifold, purge, exhaust gas recirculation (EGR), charge, cylinder and sensor, respectively. The ambient pressure and temperature, intake manifold pressure and temperature, and exhaust gas AFR are available as in general production EMS.

In this work, it is assumed that either a purge valve or EGR valve opens for simplicity, although the model and observers can be extended with minor modifications when both EGR and purge valves open. Thus, the EGR flow will not be considered hereafter. Based on the assumption, two incoming flows and one outgoing flow to/out of the intake manifold during purge events are given by

$$W_{th} = A_{th}(u_{th})\frac{p_a}{\sqrt{RT_a}}\Psi\left(\frac{p_m}{p_a}\right) \tag{1}$$

$$W_p = A_p(u_p)\frac{p_a}{\sqrt{RT_a}}\Psi\left(\frac{p_m}{p_a}\right) \tag{2}$$

$$W_c = \eta\frac{N_e V_d}{120}\frac{p_m}{RT_m} \tag{3}$$

where A_{th} and A_p are the effective area of the throttle valve and purge valve, respectively. R is a specific gas constant of air, N_e is the engine speed in rpm, V_d is the displacement volume and η is the volumetric efficiency, respectively. $\Psi(\cdot)$ shown in Fig. 2 indicates the flow restriction which is a function of the upstream and downstream pressure ratio: $r_p = p_{down}/p_{up}$ as

$$\Psi(r_p) = \begin{cases} r_p^{\frac{1}{\gamma}}\sqrt{\frac{2\gamma}{\gamma-1}\left(1-r_p^{\frac{\gamma-1}{\gamma}}\right)} & \text{, if } r_p > \left(\frac{2}{\gamma+1}\right)^{\frac{\gamma}{\gamma-1}} \\ \sqrt{\gamma\left(\frac{2}{\gamma+1}\right)^{\frac{\gamma+1}{\gamma-1}}} & \text{, if } r_p \le \left(\frac{2}{\gamma+1}\right)^{\frac{\gamma}{\gamma-1}} \end{cases}$$

Remark 2.1. From Fig. 2, $\partial\Psi(r_p)/\partial p_{down} \le 0$ if the upstream pressure is constant. Equivalently, the following holds.

$$(\Psi(r_{p1}) - \Psi(r_{p2}))(p_{down1} - p_{down2}) \le 0 \tag{4}$$

where p_{down1} and p_{down2} are any two downstream pressures, and $\Psi(r_{p1})$ and $\Psi(r_{p2})$ are the corresponding Ψ functions. (4) will be used in *Proof 3.2*.

Then, the intake manifold breathing dynamics is given by

$$\dot{p}_m = \frac{RT_m}{V_m}\left(W_{th} + W_p(1+\delta_p) - W_c\right) \tag{5}$$

$$\dot{\delta}_p = 0 \tag{6}$$

where δ_p is a multiplicative uncertainty of the purge flow to be estimated with the virtual dynamics, i.e. W_p is the nominal purge flow rate that may be inaccurate and $W_p(1+\delta_p)$ is the actual purge flow rate.

The dynamics of the charge fuel fraction (in mass) is given by

$$\dot{F}_c = \frac{RT_m}{P_m V_m}\left(-\left(W_{th} + W_p(1+\delta_p)\right)F_c + W_p(1+\delta_p)F_p\right) \tag{7}$$

$$\dot{F}_p = 0 \tag{8}$$

where V_m is the intake manifold volume and F_p is the uncertain purge fuel fraction to be estimated.

Since the charge fuel fraction (F_c) is not measured in production EMS, it needs to be estimated. The cylinder AFR is given by (9) and the time derivative of the exhaust gas AFR measured by an EGO sensor is given by (10).

$$AFR_{cyl} = \frac{W_c(1-F_c)}{W_c F_c + W_f} \tag{9}$$

$$\frac{dAFR_s}{dt} = \frac{1}{\tau_s}\left(-AFR_s + AFR_{cyl}(t-t_d)\right) \tag{10}$$

τ_s is a time constant and t_d is a time delay including a cycle delay and transport delay that depend on the engine speed and exhaust gas velocity, respectively. And W_f is the fuel flow rate. Neglecting the sensor dynamics yields a simple estimation of the charge fuel fraction as

$$F_c = \frac{W_c - W_f AFR_s}{(1+AFR_s)W_c} \tag{11}$$

3. OBSERVER DESIGN

Since the intake manifold breathing dynamics of (5) and (6) affects the charge fuel fraction dynamics of (7) and (8) in one-way, two Luenberger-like UIOs are derived sequentially assuming faster convergence of the first observer estimating the uncertain purge flow rate than the second observer estimating the uncertain purge gas fuel fraction.

3.1 Uncertain Purge Flow Rate Estimation

Consider the first Luenberger-like UIO of (12) and (13).

$$\dot{\hat{p}}_m = \frac{RT_m}{V_m}\left(\hat{W}_{th} + \hat{W}_p(1+\hat{\delta}_p) - \hat{W}_c\right) \tag{12}$$

$$\dot{\hat{\delta}}_p = L_1(p_m - \hat{p}_m) \tag{13}$$

where $\hat{\cdot}$ indicates estimation from the observer. The estimated gas flows are given by

$$\hat{W}_{th} = A_{th}(u_{th})\frac{p_a}{\sqrt{RT_a}}\Psi\left(\frac{\hat{p}_m}{p_a}\right) \tag{14}$$

$$\hat{W}_p = A_p(u_p)\frac{p_a}{\sqrt{RT_a}}\Psi\left(\frac{\hat{p}_m}{p_a}\right) \tag{15}$$

$$\hat{W}_c = \eta\frac{N_e V_d}{120}\frac{\hat{p}_m}{RT_m} \tag{16}$$

respectively.

Proposition 3.1. The observer given by (12) and (13) ensures asymptotic convergence of the estimation errors to zero for the breathing dynamics of (5) and (6) with the observer gain L_1:

$$L_1 = l_1\frac{RT_m}{V_m}W_p \tag{17}$$

where l_1 is a positive constant determining the convergence rate.

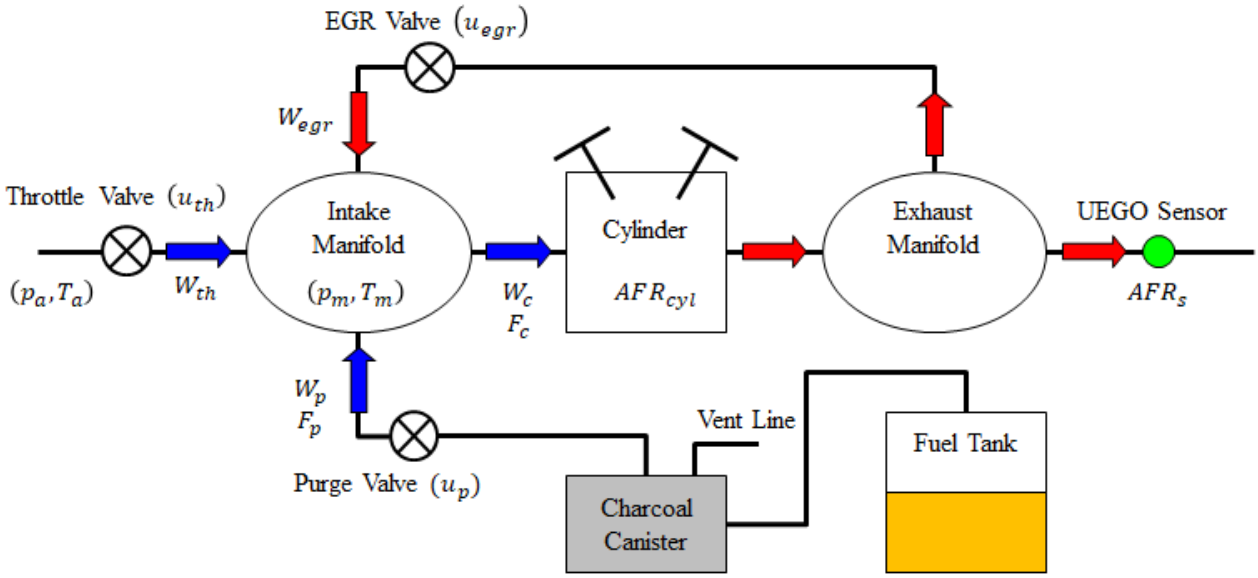

Fig. 1. Schematic of an internal combustion engine with an evaporative emission system.

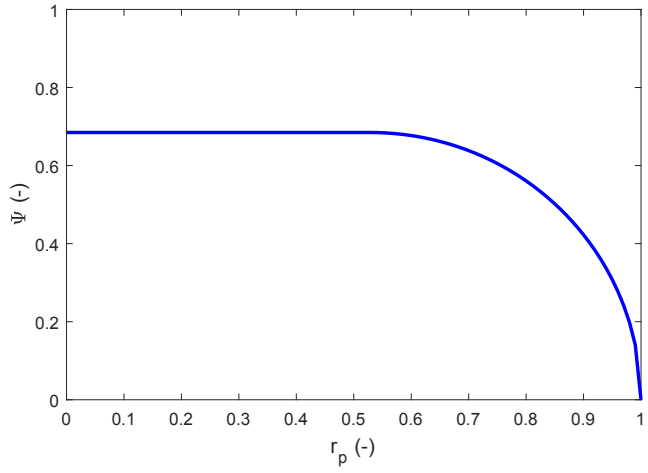

Fig. 2. Ψ function with the pressure ratio.

Proof 3.1. The estimation errors are defined as

$$\tilde{p}_m = p_m - \hat{p}_m \tag{18}$$

$$\tilde{\delta}_p = \delta_p - \hat{\delta}_p \tag{19}$$

Then, the error dynamics are given by

$$\begin{aligned}\dot{\tilde{p}}_m = \frac{RT_m}{V_m}\Bigg(&A_{th}(u_{th})\frac{p_a}{\sqrt{RT_a}}\left(\Psi\left(\frac{p_m}{p_a}\right)-\Psi\left(\frac{\hat{p}_m}{p_a}\right)\right)+W_p\tilde{\delta}_p\\&+A_p(u_p)\frac{p_a}{\sqrt{RT_a}}\left(\Psi\left(\frac{p_m}{p_a}\right)-\Psi\left(\frac{\hat{p}_m}{p_a}\right)\right)\left(1+\hat{\delta}_p\right)\\&-\eta\frac{N_eV_d}{120}\frac{1}{RT_m}\tilde{p}_m\Bigg)\end{aligned} \tag{20}$$

$$\dot{\tilde{\delta}}_p = -L_1\tilde{p}_m \tag{21}$$

A Lyapunov function candidate is defined as

$$V = \frac{c_1}{2}\tilde{p}_m^2 + \frac{c_2}{2}\tilde{\delta}_p^2 \tag{22}$$

where c_1 and c_2 are positive constants. Then, the time derivative of the Lyapunov function candidate is given by

$$\begin{aligned}\dot{V} = c_1\frac{RT_m}{V_m}\Bigg(&A_{th}(u_{th})\frac{p_a}{\sqrt{RT_a}}\left(\Psi\left(\frac{p_m}{p_a}\right)-\Psi\left(\frac{\hat{p}_m}{p_a}\right)\right)\tilde{p}_m\\&+W_p\tilde{p}_m\tilde{\delta}_p\\&+A_p(u_p)\frac{p_a}{\sqrt{RT_a}}\left(\Psi\left(\frac{p_m}{p_a}\right)-\Psi\left(\frac{\hat{p}_m}{p_a}\right)\right)\tilde{p}_m\left(1+\hat{\delta}_p\right)\\&-\eta\frac{N_eV_d}{120}\frac{1}{RT_m}\tilde{p}_m^2\Bigg)-c_2L_1\tilde{p}_m\tilde{\delta}_p\end{aligned} \tag{23}$$

Note that since $(\Psi(p_m/p_a)-\Psi(\hat{p}_m/p_a))\tilde{p}_m \le 0$ by *Remark 2.1*, the first and third terms in the big bracket are non-positive. Thus, with the observer gain of (17) where $l_1 = c_1/c_2$,

$$\dot{V} \le -\eta\frac{N_eV_d}{120}\frac{1}{RT_m}\tilde{p}_m^2 \le 0$$

Then, by LaSalle's invariant principle in Hassan (2002), the estimation errors converge to zero asymptotically. □

3.2 Unknown Purge Gas Fuel Fraction Estimation

Based on the assumption of faster convergence rate of (12) and (13), (7) is rewritten by

$$\dot{F}_c = \frac{RT_m}{P_mV_m}\left(-\left(\hat{W}_{th}+\hat{W}_p\left(1+\hat{\delta}_p\right)\right)F_c+\hat{W}_p\left(1+\hat{\delta}_p\right)F_p\right) \tag{24}$$

Then, consider the second Luenberger-like UIO of (25) and (26).

$$\dot{\hat{F}}_c = \frac{RT_m}{p_mV_m}\left(-\left(\hat{W}_{th}+\hat{W}_p\left(1+\hat{\delta}_p\right)\right)\hat{F}_c+\hat{W}_p\left(1+\hat{\delta}_p\right)\hat{F}_p\right) \tag{25}$$

$$\dot{\hat{F}}_p = L_2(F_c - \hat{F}_c) \tag{26}$$

Proposition 3.2. The observer of (25) and (26) ensures asymptotic convergence of the estimation errors to zero for the fuel fraction dynamics of (24) and (8) with the observer gain L_2:

$$L_2 = l_2\frac{RT_m}{p_mV_m}\hat{W}_p(1+\hat{\delta}_p) \tag{27}$$

where l_2 is a positive constant.

Proof 3.2. The estimation errors are defined as:

$$\tilde{F}_c = F_c - \hat{F}_c \tag{28}$$

$$\tilde{F}_p = F_p - \hat{F}_p \tag{29}$$

Then, the error dynamics are given by

$$\dot{\tilde{F}}_c = \frac{RT_m}{p_m V_m}\left(-\left(\hat{W}_{th} + \hat{W}_p\left(1+\hat{\delta}_p\right)\right)\tilde{F}_c + \hat{W}_p\left(1+\hat{\delta}_p\right)\tilde{F}_p\right) \tag{30}$$

$$\dot{\tilde{F}}_p = -L_2\tilde{F}_c \tag{31}$$

A Lyapunov function candidate is defined as

$$V = \frac{c_3}{2}\tilde{F}_c^2 + \frac{c_4}{2}\tilde{F}_p^2 \tag{32}$$

where c_3 and c_4 are positive constants. Then, the time derivative of the Lyapunov function candidate is given by

$$\dot{V} = c_3\frac{RT_m}{p_m V_m}\left(-\left(\hat{W}_{th} + \hat{W}_p\left(1+\hat{\delta}_p\right)\right)\tilde{F}_c^2 + \hat{W}_p\left(1+\hat{\delta}_p\right)\tilde{F}_c\tilde{F}_p\right) - c_4 L_2\tilde{F}_c\tilde{F}_p \tag{33}$$

Using the observer gain of (27) where $l_2 = c_3/c_4$,

$$\dot{V} \leq -c_3\frac{RT_m}{p_m V_m}\left(\hat{W}_{th} + \hat{W}_p\left(1+\hat{\delta}_p\right)\right)\tilde{F}_c^2 \leq 0$$

Similarly, by LaSalle's invariant principle, the estimation errors converge to zero asymptotically. □

3.3 Application to AFR Control

In general production EMS, the fuel flow rate is determined by a feedforward control and feedback control as

$$W_f = W_f^{ff} + W_f^{fb} \tag{34}$$

The feedforward control is determined by the air flow rate estimation of charge gas and the stoichiometric AFR value, i.e. $W_f^{ff} = \hat{W}_c/AFR_{st}$, and the feedback control is a proportional-integral (PI) control taking an universal or heated exhaust gas oxygen (UEGO or HEGO) sensor signal as a feedback. Typically, feedback control gains are tuned at different operational conditions regarding identified parameter-varying sensor dynamics of (10) such as Postma and Nagamune (2010). Note that detailed design and calibration of the feedback control is not a scope of this work.

To improve robustness of the AFR control with reduced calibration effort while purge comes into play, it is desired to estimate and compensate for uncertainties that bring negative effects to the AFR control. Toward this end, Yoo et al. (1999); Aswani et al. (2009); Zamanian et al. (2014) developed different feedforward control methods based on purge estimation. In this work, the feedforward control based on the estimated charge fuel fraction ($\hat{F}_c$) is proposed as

$$W_f^{ff} = (1-\hat{F}_c)\frac{\hat{W}_c}{AFR_{st}} \tag{35}$$

The amount of fuel to be injected is reduced as much as the estimated fuel amount in charge gas. It is noted that since $\hat{F}_c$ of (25) and (26) is in a feedback control structure, (35) can be interpreted as a combination of the nominal feedforward control and implicit feedback control. If the purge valve closes, i.e. $\hat{W}_p = 0$, $\hat{F}_c$ will converge to zero, and consequently this implicit feedback will also converge to zero. Other uncertainties such as transient and injector tolerance must be compensated by the explicit PI feedback control W_f^{fb}.

4. NUMERICAL VALIDATION

The well-tuned and map-based spark-ignition gasoline engine model of 1.5 liter available in MATLAB & Simulink (2021) was employed for numerical validation of the developed observers. Fig. 3 and 4 show the calibrations for the throttle valve area and volumetric efficiency map, respectively. Note that the UEGO sensor dynamics of (10) is included in the simulation model, although it is neglected in the observer design.

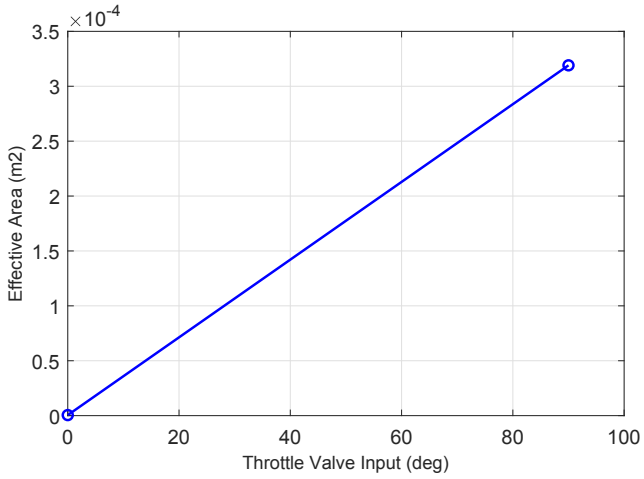

Fig. 3. Effective throttle valve area

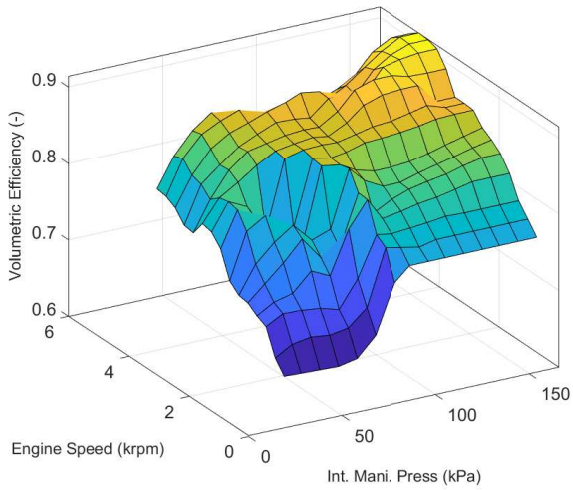

Fig. 4. Volumetric efficiency map

Fig. 5 shows the simulated engine operational condition extracted from the federal test procedure driving cycle (FTP-75). It includes idle and transient with aggressive purge up to 45 % purge valve opening.

Fig. 6 shows the simulated uncertainties on the purge valve area calibration and unknown purge fuel fraction, respectively. The highest uncertainty at low purge valve opening is assumed to represent uncertain turbulence with small purge valve area. High purge fuel fraction is assumed initially, and reduces gradually due to depletion of vapor fuel during aggressive purge.

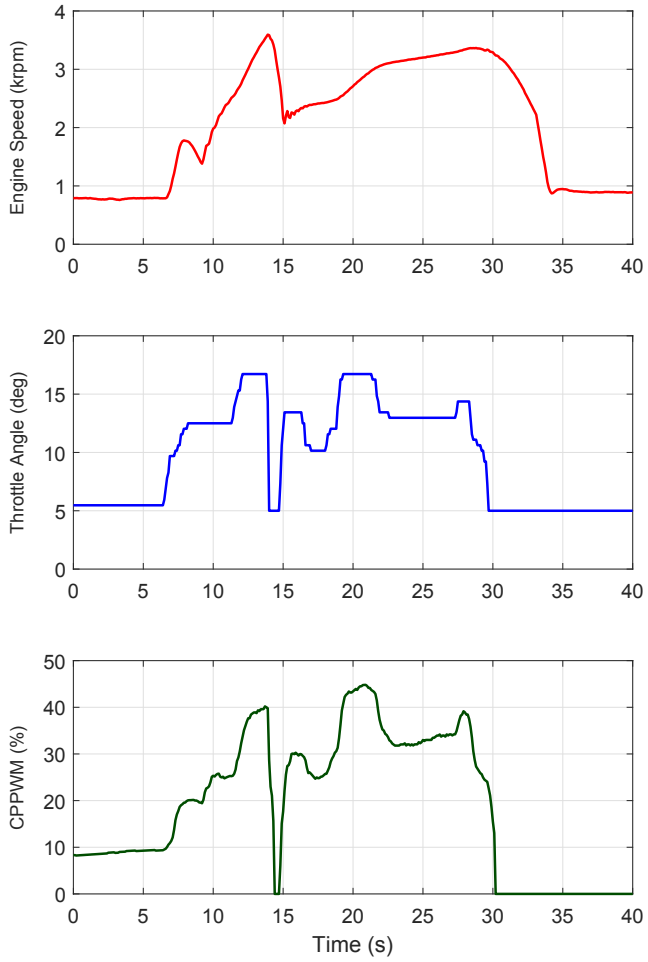

Fig. 5. Simulated engine operational condition: engine speed in krpm; throttle valve opening in degree; canister purge valve pulse width modulation (CPPWM) signal in percent.

Fig. 7 shows the estimated throttle flow, charge flow, intake manifold pressure, and purge flow. They converge to the actual values quickly and accurately. Fig. 8 shows the estimated fuel fraction of charge gas and purge gas. They also show good convergence although some excursions of the purge fuel fraction estimation attributable to neglecting sensor dynamics are observed near 15 seconds and after 30 seconds, but still these excursions are in the acceptable range.

Fig. 9 shows the simulated AFR using the feedforward control only. The solid green, dashed blue, and dashed-dotted red are the stoichiometric AFR, AFR without purge correction, and AFR with purge correction, respectively. It turns out that even without the (explicit) feedback control, the proposed feedforward control can reject the negative effect of aggressive vapor purge on AFR. It is noted that the purged fuel can be considered as an uncertain disturbance and compensated by the feedback control as in Ebrahimi et al. (2012). However, it requires significant calibration effort and it may limit aggressive purge due to complexity of on-board diagnostics of an EVAP system, Grieve and Himes (2000).

5. CONCLUSION

In this paper, an observer-based purge estimation method is developed for a robust AFR control of gasoline engines. Based on physical models of the intake manifold breathing dynamics

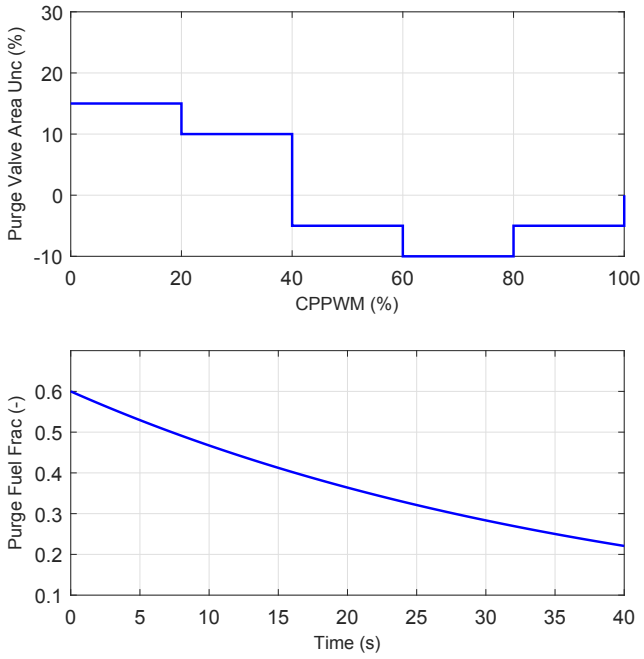

Fig. 6. Simulated uncertainties: uncertainty of the canister purge valve effective area (upper); unknown fuel fraction of the purged gas (lower).

and charge fuel fraction dynamics, the sequential Luenberger-like unknown input observers are derived and their convergence properties are investigated analytically and numerically. Based on the charge fuel fraction estimation, a novel feedforward AFR control is proposed and numerically demonstrated. It reveals great potential for improving robustness of an AFR control. In the observer design, the sensor dynamics including a time delay is neglected, which may negatively affect observer convergence. Robust observer design taking a delayed AFR measurement into account is a future work to be conducted.

REFERENCES

Andersson, P. and Eriksson, L. (2005). Observer based Feedforward Air-Fuel Control of Turbocharged SI-Engines. In *IFAC World Congress*, 200–205. July, Prague, Czech Republic.

Aswani, D., Cook, J., Larkin, R., and Kuechler, P. (2009). Vapor Purge Estimation using a Dual-Mode Observer. *Control Engineering Practice*, 17(8), 864–873.

Corvino, C., Oliva, A., and Zanasi, R. (2014). Carbon Canister Air Fuel Ratio Estimation on High Performance Engine. In *Mediterranean Conference on Control and Automation*, 30–36. Palermo, Italy.

Ebrahimi, B., Tafreshi, R., Masudi, H., Franchek, M., Mohammadpour, J., and Grigoriadis, K. (2012). A Parameter-Varying Filtered PID Strategy for Air-Fuel Ratio Control of Spark Ignition Engines. *Control Engineering Practice*, 20(8), 805–815.

Goto, O., Uozumi, Y., and Watanabe, M. (1982). Evaporative Emission Control System for an Internal Combustion Engine. URL `https://www.osti.gov/biblio/5584948`. US Patent 4308842.

Grieve, M.J. and Himes, E.G. (2000). Advanced Canister Purge Algorithm with a Virtual [HC] sensor. *SAE Technical Paper*, 615–621. 2000-01-0557.

Hassan, K.K. (2002). *Nonlinear Systems*. Prentice Hall, Upper Saddle River, NJ.

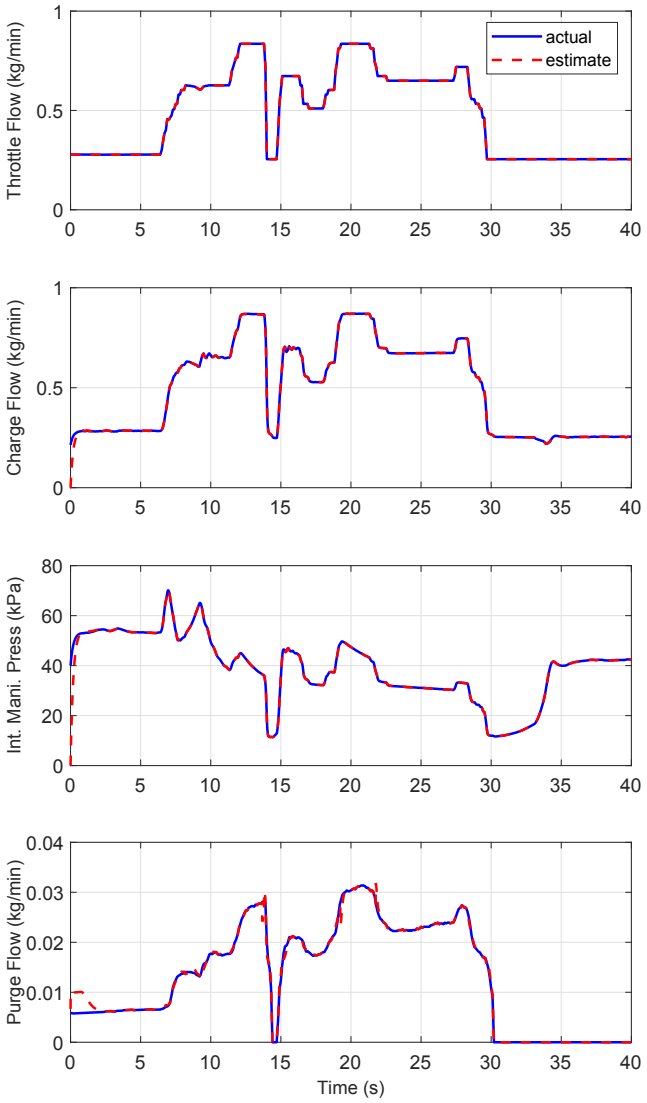

(a)

Fig. 7. Uncertain purge flow rate estimation results

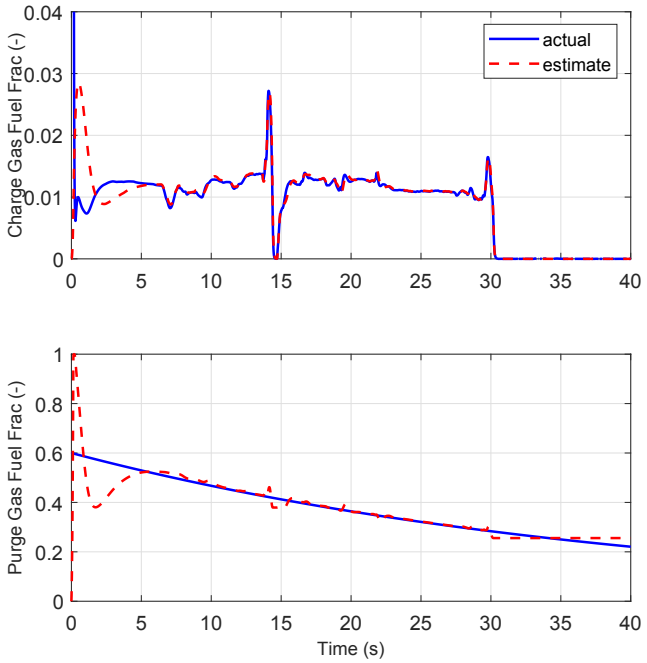

Fig. 8. Uncertain purge fuel fraction estimation results.

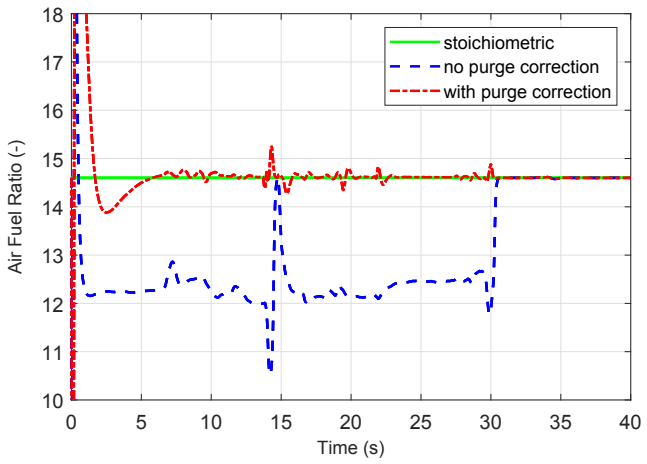

Fig. 9. AFR with the feedforward fuel control only: stoichiometric (solid green), without purge correction (dashed blue), with purge correction (dashed-dotted red).

Hassani Monir, V., Salehi, R., Salarieh, H., Alasty, A., and Vossoughi, G. (2015). Real-time Estimation of the Volumetric Efficiency in Spark Ignition Engines using an Adaptive Sliding Mode Observer. *Proceedings of the Institution of Mechanical Engineers, Part D: Journal of Automobile Engineering*, 229(14), 1925–1933.

Heywood, J.B. (1998). *Internal Combustion Engine Fundamentals*. McGraw-Hill, New York.

Leroy, T., Chauvin, J., Le Solliec, G., and Corde, G. (2007). Air Path Estimation for a Turbocharged SI Engine with Variable Valve Timing. In *American Control Conference*, 5088–5093. July, New York, USA.

MATLAB & Simulink (2021). Internal Combustion Engine Reference Application Projects. `https://www.mathworks.com/help/autoblks/ug/si-engine-project-template.html`.

Postma, M.J. and Nagamune, R. (2010). LPV-Based Air-Fuel Ratio Control of Spark Ignition Engines Using Two Gain Scheduling Parameters. In *Dynamic Systems and Control Conference*, 665–672. Cambridge, MA, USA.

Stotsky, A. and Kolmanovsky, I. (2002). Application of Input Estimation Techniques to Charge Estimation and Control in Automotive Engines. *Control Engineering Practice*, 10(12), 1371–1383.

Wang, Z., Zhu, Q., and Prucka, R. (2016). A Review of Spark-Ignition Engine Air Charge Estimation Methods. *SAE Technical Paper*. 2016-01-0620.

Yoo, I.K., Upadhyay, D., Kim, Y.W., and Rizzoni, G. (1999). An Application of Carbon Canister Modeling to Air Fuel Ratio Control and Idle By-Pass Control. *SAE Technical Paper*. 1999-01-1093.

Zamanian, F., Franchek, M.A., Grigoriadis, K.M., and Makki, I. (2014). Steady State Fueling Compensation for Purge Control in Internal Combustion Engines. In *American Control Conference*, 855–860. Portland, OR, USA.